Physica B: Condensed Matter 545 (2018) 222–227

Contents lists available at ScienceDirect

Physica B: Condensed Matter

journal homepage: www.elsevier.com/locate/physb

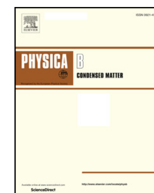

Electric field effect on variable-range hopping conductivity in $Bi_{1.9}Lu_{0.1}Te_3$

Oleg Ivanov[a,*], Maxim Yaprintsev[a], Elena Danshina[b]

[a] Belgorod State University, Belgorod, 308015, Russian Federation
[b] Belgorod State Technological University named after V.G. Shukhov, Belgorod, 308012, Russian Federation

ARTICLE INFO

Keywords:
Variable-range hopping conductivity
Average hopping distance
Electric field activation
Density of states

ABSTRACT

Electric field effect on low-temperature electrical resistivity of *n*-type $Bi_{1.9}Lu_{0.1}Te_3$ was examined and analyzed. It was found that with decreasing temperature from 35 down to 2.5 K, the conductivity mechanism changes from "metal" type to "semiconductor" one resulting in appearance of minimum in the specific electrical resistivity, ρ. The temperature of this minimum, T_m, depends on electric field strength, *E*. At low electric field of 0.15 V·m^{-1} this temperature is equal to ∼11 K and decreases as *E* increases up to 4.65 V·m^{-1}. Variable-range hopping (VRH) conductivity mechanism was applied to explain the ρ(*T*, *E*) behavior below T_m. Average hopping distance estimated from the experimental ρ(*T*, *E*) dependences decreases as temperature or electric field strength increase, that is the VRH conductivity can be activated both temperature and electric field. It was also found that density of states at the Fermi level rapidly enhances as electric field increases. This enhancement could be attributed to high and sharp density of states within an impurity band formed from the electronic *f*-levels of Lu. The forming of this impurity band is believed to be responsible for enhancement of the thermoelectric figure-of-merit of Bi_2Te_3.

1. Introduction

Element doping is one of promising ways to improve the thermoelectric efficiency of bismuth telluride, Bi_2Te_3, and Bi_2Te_3-based compounds [1–5]. This doping can at the same time effect on the Seebeck coefficient, *S*, the specific electrical resistivity, ρ, and the total thermal conductivity, *k*, to maximize the dimensionless thermoelectric figure-of-merit, *ZT*, defined as $(S^2/\rho k)T$, where *T* is the absolute temperature. The most effective dopants are atoms or ions of elements forming a narrow and non-parabolic impurity band lying near the Fermi level with high and sharp density of states (DOS) [6–8]. This impurity band has to lye inside or, at least, been partially overlapping with conductance (valence) band. In this case, both scattering factor and density-of-states effective mass of carriers could be remarkably enhanced resulting in an increase of the Seebeck coefficient.

Recently, it was found that rare earth elements like Lu, Ce, Sm, Er, La can enhance the thermoelectric figure-of-merit of Bi_2Te_3 [9–18]. This *ZT* enhancement can really originated from forming the narrow and non-parabolic impurity band related to rare earth elements. In accordance with theoretical predictions, an ideal electronic DOS to maximize the *ZT* value is the Dirac delta function not achievable in real solids [19,20]. However, electronic *f*-levels of rare earth elements are tightly bound in atoms, and bind little in solids forming the sharp Lorentzian singularity of very narrow width in DOS lying near the Fermi level [21]. Such kind of singularity is the closest approximation to the Dirac delta function.

Besides an increase in the Seebeck coefficient, the impurity band can remarkably effect on low temperature electrical conductivity of thermoelectrics. This effect is usually due to hopping conductivity onset as electron gets ability to tunnel from one to another localized state within the impurity energy band [22]. The hopping conductivity is characteristic of heavily doped semiconductors, which behave as strongly disordered and inhomogeneous systems.

The Seebeck coefficient enhancement due to an increase of the density-of-states effective mass of electron was earlier found in *n*-type $Bi_{1.9}Lu_{0.1}Te_3$ [23]. This enhancement is assumed to be related to the impurity (Lu) band with local maximum of electronic density of states lying near the Fermi level. Minimum in the specific electrical resistivity, ρ, originated from a change of the conductivity mechanism was also observed at temperature $T_m \approx 11$ K. Analyzing the temperature and magnetic field dependences of the electrical resistivity allowed us to conclude that the variable-range hopping (VRH) conductivity takes place in $Bi_{1.9}Lu_{0.1}Te_3$ below T_m. At the VRH conductivity, the hopping of carriers is temperature activated, yielding a *T*-dependent resistivity. Additional activation of the VRH conductivity can be provided by strong enough electric field with strength *E*, resulting in an *E*-dependent resistivity. Measuring and analyzing the temperature and electric field dependences of ρ, the average hopping distance can be estimated.

* Corresponding author. Belgorod State University, Pobedy 85, Belgorod, 308015, Russian Federation.
E-mail address: Ivanov.Oleg@bsu.edu.ru (O. Ivanov).

https://doi.org/10.1016/j.physb.2018.06.021
Received 19 February 2018; Received in revised form 11 May 2018; Accepted 19 June 2018
Available online 20 June 2018
0921-4526/ © 2018 Elsevier B.V. All rights reserved.

The purpose of this paper is to find and examine the electric field effect on the variable-range hopping conductivity in $Bi_{1.9}Lu_{0.1}Te_3$.

2. Materials and methods

The microwave-solvothermal synthesis and spark plasma sintering methods were applied to prepare the $Bi_{1.9}Lu_{0.1}Te_3$ compound. To synthesize a starting powder, analytically pure chemicals (Bi_2O_3, TeO_2, Lu_2O_3, ethylene glycol, nitric acid and N,N-dimethylformamide) were used. First, the oxides taken in a stoichiometric ratio were dissolving in mixture of concentrated nitric acid and ethylene glycol. Then, N,N-dimethylformamide was added in mixture after dissolving. Finally, the microwave-assisted reaction was carried out in a MARS-6 microwave reactor at pressure of 4 MPa, temperature of 463 K for 15 min. To sinter the bulk $Bi_{1.9}Lu_{0.1}Te_3$ samples, the park plasma sintering method was applied by using a SPS-25/10 system at pressure of 40 MPa, temperature of 683 K and sintering time of 5 min.

To determine a phase composition of the bulk samples, X-ray diffraction (XRD) analysis was performed by a Rigaku Ultima IV diffractometer with CuK_α – radiation. The XRD pattern was found to be in agreement with the rhombohedral $R\bar{3}m$ symmetry characteristic of Bi_2Te_3 and no remarkable impure phases such as tellurium, bismuth, lutetium or their other compounds were observed.

A scanning electron microscope (SEM), Nova NanoSEM 450, was also applied to examine grain structure of the bulk samples.

To determine a correct elemental composition of materials prepared, a Shimadzu ICP (Inductively Coupled Plasma) emission spectrometer ICPE-9000 was applied. As wastage and volatilization are unavoidable during spark plasma sintering, the real composition may deviate from the nominal one. However, according to analysis results, the Bi, Te and Lu content was equal to 38.07 at%, 59.95 at% and 1.98 at %, respectively. That is the content of these elements really corresponds to the $Bi_{1.9}Lu_{0.1}Te_3$ composition and the atomic (Bi + Lu)/Te ratio is equal to 2/3.

To measure the specific electrical resistivity, the rectangular bar samples with dimensions of $0.5 \times 0.5 \times 5\ mm^3$ were used. Opposite faces of the bar perpendicular to a long side were covered by silver paste and a voltage drop across these faces was measured. Mini Cryogen Free Measurements System (Cryogenic Ltd, UK) was applied to take the ρ(*T*) dependences at various values of a current density, *j*. The *j* values were equal to $9{\cdot}10^4$, $29{\cdot}10^4$, $44{\cdot}10^4$, $88{\cdot}10^4$, $177{\cdot}10^4$ and $280{\cdot}10^4$ $A{\cdot}m^{-2}$. Then, using the ρ value of the sample studied, the electric field strengths corresponding to these currents could be calculated by the Ohm law. The value ρ = 1.66 μΩ·m was taken to calculate *E*. In addition, taking into account a weak temperature dependence of the specific electrical resistivity within a temperature range chosen, *E* is believed to be *T*-independent. So, the calculated *E* values were equal to ~0.15, 0.48, 0.73, 1.46, 2.94 and 4.65 $V{\cdot}m^{-1}$.

3. Results and discussion

The temperature dependences of the specific electrical resistivity of $Bi_{1.9}Lu_{0.1}Te_3$ taken for the temperature 2.5–35 K range and at the electric field strengths of 0.15 and 4.65 $V{\cdot}m^{-1}$ are shown in Fig. 1 (a). First of all, one can see that for whole temperature range ρ decreases as *E* increases. Further, taking into account a quite different behavior of the ρ(*T*) dependences for these both electric fields, two regimes of the *E*-effect on the specific electrical resistivity corresponding to weak or strong electric field would be reasonably considered. Clear minimum in the ρ(*T*) dependence centered at temperature $T_m \approx 11$ K is observed for weak electric field of 0.15 $V{\cdot}m^{-1}$, while this minimum is totally depressed at strong electric field of 4.65 $V{\cdot}m^{-1}$. Besides, an efficiency of the *E*-effect on ρ is *T*-dependent. To demonstrate this temperature effect in detail, the ρ(*T*) dependence for weak electric field should be subtracted from ρ(*T*) dependence for strong electric field. The temperature dependence of this ρ difference, Δρ, is shown in Fig. 1 (b). At cooling, Δρ gradually increases from zero at the highest temperature of 35 K up to 0.01 μΩ·m at the lowest temperature of 2.5 K. So, the *E*-effect on ρ is enhancing as temperature decreases.

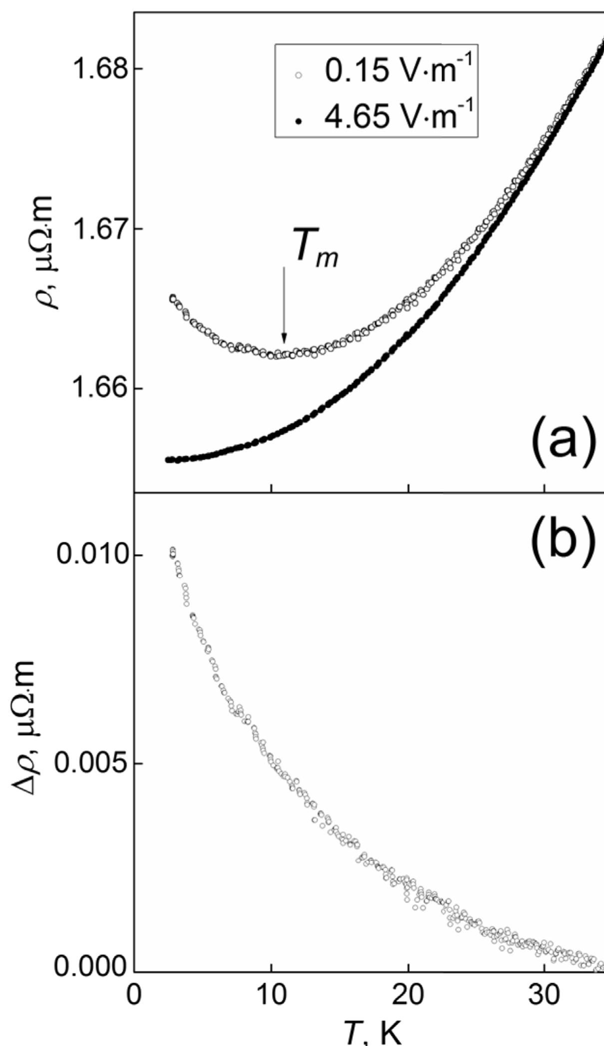

Fig. 1. The ρ vs. *T* dependences at weak (0.15 $V{\cdot}m^{-1}$) and strong (4.65 $V{\cdot}m^{-1}$) electric fields (a) and the Δρ vs. *T* dependence (b).

Appearance of the ρ(*T*) minimum at T_m for weak electric field can be originated from a change of the conductivity mechanism. Above T_m this mechanism is characteristic of metals (ρ increases as *T* increases), while below T_m the ρ(*T*) dependence is corresponding to semiconductors (ρ decreases as *T* increases). In turn, the ρ(*T*) dependence for strong electric field is rather characterized by one "metal" conductivity mechanism, because ρ gradually decreases and obviously tends to some saturated value as temperature approaches to 0 K.

The depression of the "semiconductor" conductivity mechanism at gradual *E* increase is shown in Fig. 2 (b). The ρ(*T*) minimum is gradually depressed and shifted to lower temperatures as *E* increases from 0.15 to 1.46 $V{\cdot}m^{-1}$. Just high-temperature part of the ρ(*T*) minimum is observed for *E* equal 2.94 $V{\cdot}m^{-1}$ and no ρ minimum can be found for the highest electric field of 4.65 $V{\cdot}m^{-1}$.

To correctly determine the T_m values in Fig. 2 (a) and recovery the $T_m(E)$ curve, the derivatives *d*ρ/*dT* versus *T* dependences were plotted for various *E* values. This dependence for $E = 1.46\ V{\cdot}m^{-1}$ is shown in Fig. 2 (b). The temperature T_m obviously corresponds to such temperature at which the derivative *d*ρ/*dT* changes its sign. Inset to Fig. 2 (b) shows the $T_m(E)$ curve. The temperature T_m slightly decreases at $E \leq 0.73\ V{\cdot}m^{-1}$, but rapidly drops at higher electric fields. This tendency is in agreement with the Δρ(*T*) dependence presented in Fig. 1

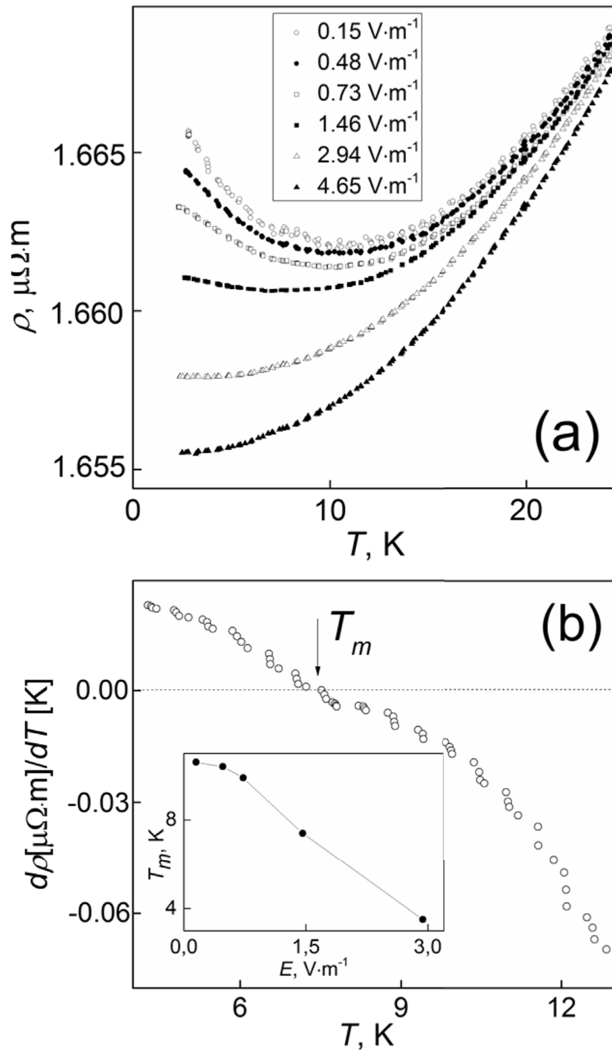

Fig. 2. The ρ vs. T dependences at various electric fields (a) and the $d\rho/dT$ vs. T dependence for $E = 1.46\ \mathrm{V{\cdot}m^{-1}}$ (b). Inset: the $T_m(E)$ dependence.

(b).

Now let us analyze the mechanisms of the E-effect on ρ in $Bi_{1.9}Lu_{0.1}Te_3$. As was mentioned above, the ρ(T) minimum at T_m for weak electric field can be originated from a change of the conductivity mechanism from a "metal" conductivity above T_m to "semiconductor" conductivity below T_m. As was recently reported [23], the variable-range hopping conductivity can take place in $Bi_{1.9}Lu_{0.1}Te_3$ below T_m. In this case, the impurity (Lu) energy band is believed to be responsible for the conductivity of this compound. At high temperatures, the electrons within this impurity band are delocalized and $Bi_{1.9}Lu_{0.1}Te_3$ behaves as metal or degenerate semiconductor, but at low temperatures a weak localization of carriers and, hence, a transition to the VRH conductivity can occur.

Generally, there are the nearest neighbor hopping conductivity (NNH) and VRH conductivity [22]. The NNH conductivity is the hopping conductivity in which the electron in an initial localized state obtains the energy and hops to a nearest localizes state. The NNH conductivity is limited by the thermal energy of the electrons. When the temperature is very low, a probability of the electron thermal activation between states that are close in space but far in energy becomes smaller than that of electron hopping between some more remote states whose energy levels happen to be very close each to other. In this case, the average hopping distance increases as temperature decreases. The VRH conductivity sets in when the internal microscopic disorder is high enough to make tunneling between the nearest sites energetically unfavorable.

It is known [22] that the elementary hopping process can be either a phonon-assisted tunneling through the potential barrier between two localized states or a thermally activated jump over this barrier. The tunneling probability is related to the overlap in the wave functions of the localized states, ψ, and the wave function itself exponentially decays from the centre as

$$\Psi(r) \sim \exp(-\alpha r), \tag{1}$$

where α is the spatial extent measure of the wave function.

The over barrier hopping probability is determined by the Boltzmann factor, exp(- W/k_BT), where W is the energy difference between two localizes states. Finally, the probability of the electron to hop from one localized state to another one, ω, taking into account both tunneling term and thermally activated term is expressed as

$$\omega = \omega_0 \exp\left(-2\alpha l - \frac{W}{k_B T}\right), \tag{2}$$

where ω_0 is the quantity depending on the phonon spectrum and l is the inter-states distance or the average hopping distance.

The variable-range hopping conductivity in three dimensional doped crystalline semiconductors can be described by a universal equation [24]

$$\rho(T) = AT^q \exp\left[\left(\frac{T_0}{T}\right)^p\right], \tag{3}$$

where A is the constant, T_0 is the characteristic temperature, p and q are the exponents depending on the regime of the hopping conductivity.

The experimental ρ(T) dependence of $Bi_{1.9}Lu_{0.1}Te_3$ below T_m was earlier described by expression (3) with $p = 1/4$ and $q = -3/4$ [23]. Such p value is characteristic of the VRH conductivity of the Mott type, and such q value is related to wave function of the localized states expressed as [25]

$$\psi(r) \sim r^{-1} \exp(-\alpha r). \tag{4}$$

Expression (3) takes into account an electron energy change due to temperature change and neglects an electron energy change due to electric field. This approach can be used at not very low temperatures and weak enough electric fields. The thermal energy available to the electron is k_BT, where k_B is the Boltzmann constant. In applied electric field with strength E the electron gains an additional energy, $e\varepsilon El$, where e and ε are the unit of charge and relative dielectric constant, respectively. It is important to note that the temperature and electric field activation are interchangeable. In accordance with the approach proposed in Ref. [26], let us take into account both thermal and electric field activation in expression (3) with $p = 1/4$ and $q = -3/4$ as follows

$$\rho(T) = AT^{-3/4} \exp\left[\left(\frac{k_B T_0}{k_B T + e\varepsilon El}\right)^{1/4}\right]. \tag{5}$$

Now the second activation mechanism due to electric field activation and additional to the thermal activation will also determine the VRH conductivity.

The characteristic temperature T_0 can be expressed as

$$T_0 = \frac{\lambda^4 \alpha l^3}{k_B g(F)}, \tag{6}$$

where $g(F)$ is the density of states at the Fermi level and λ is the constant equal to 2.05 [22].

The temperature T_0 also characterizes the temperature dependence of the average hopping distance as follows

$$l = \frac{3}{4}\left(\frac{T_0}{T}\right)^{1/4} \alpha^{-1}. \tag{7}$$

Let us apply expression (5) to analyze the E-effect on the ρ(T)

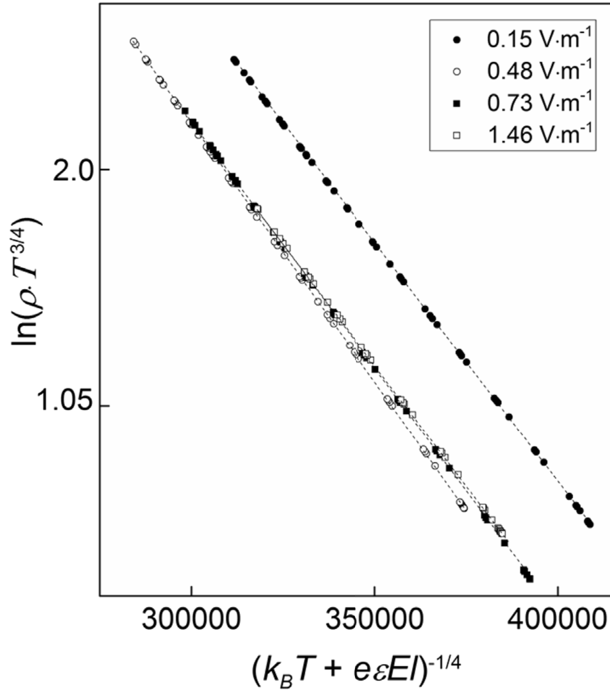

Fig. 3. The $\ln(\rho{\cdot}T^{3/4})$ vs. $(k_B + e\varepsilon El)^{-1/4}$ dependences at various electric fields.

dependences presented in Fig. 2 (a). We will use the ε value equal to 290 as reported for Bi_2Te_3 at 15 K [27]. In this case, l is a fitting parameter depending on both T and E, that is $l = l\ (T, E)$. We will also believe that the $l(T)$ dependence obeys expression (7).

In accordance with expression (5), the experimental $\rho(T)$ curves taken below T_m were replotted as the $\ln(\rho{\cdot}T^{3/4})$ versus $(k_B + e\varepsilon El)^{-1/4}$ dependences. Fig. 3 shows these dependences for $E = 0.15$, 0.48, 0.73 and 1.46 V·m^{-1}.

One can see that expression (5) very well fits the experimental $\rho(T)$ curves at various electric fields. The $l(T, E)$ values were extracted from the fitting lines in Fig. 3. The $l(T)$ dependences at various E recovered by the fitting are presented in Fig. 4. Here, the $l(T)$ changes obeying expression (7) were used as one of the fitting conditions. Inset to Fig. 4 shows $l(E)$ dependences at temperatures of 2.8 and 6.5 K. The average hopping distance decreases as temperature or electric field increase. These T- and E-effects on l are more pronounced at low temperatures and weak electric fields. To account for this $l(T, E)$ behavior, an explanation proposed in Ref. [26] may be applied.

For low activation energy that is at low temperatures and weak electric fields, the electron has to travel a long way to get some final localized state with the energy close enough to the energy of the initial localized state. As activation energy increases that is at high temperatures and strong electric fields, the range of accessible energies of the final localized states broadens. Now, more states near the initial localized state become available for the electron hops. So, the average hopping distance will decrease. In other words, at low temperatures and weak electric field, the small current is carried by a few electron hops over a long distance, while at high temperatures and strong electric field more current is carried by more hops over a shorter distance.

The slope of the lines in Fig. 3 can be used to estimate the T_0 values for various electric fields. Then, using these T_0 values and $l(T)$ dependences in Fig. 4, expression (7) was applied to also estimate the l values. Finally, the density of states at the Fermi level was estimated by expression (6), too. The T_0, α, $g(E_F)$ estimates together with the l estimates at temperatures of 2.8 and 6.5 K are listed in Table 1.

The α value remarkably increases as electric field increases. This tendency corresponding to the l decrease is in agreement with expression (2). The most interesting behavior was found in the $g(F)$ versus E

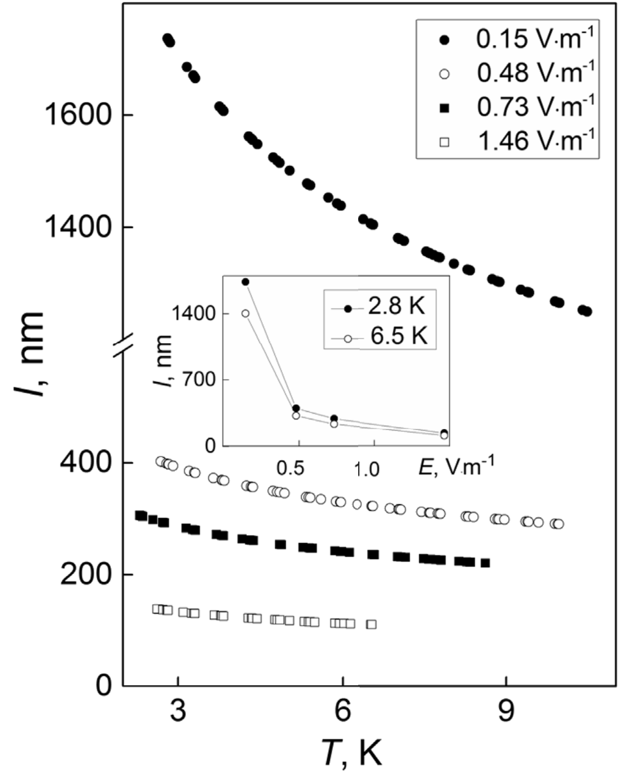

Fig. 4. The a vs. T dependences at various electric fields. Inset: the $a(E)$ dependences at temperatures of 2.8 and 6.5 K.

Table 1
The l, T_0, α and $g(E_F)$ parameters calculated for the VRH conductivity analysis.

E, V·m^{-1}	l, 10^{-9}, m (at 2.8/6.5 K)	T_0, K	α, 10^6, m^{-1}	$g(F)$, m^{-3}·eV^{-1}
0.15	1730/1400	750	1.74	$14.40{\cdot}10^{20}$
0.48	400/320	1020	8.20	$1.11{\cdot}10^{23}$
0.73	290/240	860	10.70	$2.92{\cdot}10^{23}$
1.46	135/110	810	23.40	$3.20{\cdot}10^{24}$

dependence. At weak electric field of 0.15 V·m^{-1} the density of states is very low, but $g(F)$ very fast increases as E increases up to 1.46 V·m^{-1}. This feature can be related to high and sharp density of states in the impurity band. As was mentioned above, the electronic f-levels of rare earth elements can really form the sharp Lorentzian singularity of very narrow width in DOS near the Fermi level [21]. In this case, even a slight increase of the electron energy via electric field activation could result in sufficient change of $g(F)$.

Finally, let us compare the estimated l values with some specific sizes controlling the VRH conductivity. First of all, one can believe that the maximum l value should be limited by the grain size. To estimate the grain size of the bulk $Bi_{1.9}Lu_{0.1}Te_3$ sample, the SEM image of the grain structure recorded on the fractured surfaces was analyzed. Disordered grain structure with the grains having a crystal faceting can be found in Fig. 5 (a). To estimate the average grain size, $\overline{D}$, the histogram of the grain size distribution was plotted (Fig. 5 (b)). The sizes, D, of more than 100 grains were measured on the SEM image to obtain the reliable size distribution. The grain size distribution was discretized by dividing into the 0.5 μm - width segments. This histogram can be described by a lognormal unimodal distribution. The lognormal probability density function can be expressed as [28]

$$P(d) = \frac{1}{\sqrt{2\pi}\sigma D}\exp\left(-\frac{(\ln d - \ln\overline{D})^2}{2\sigma^2}\right), \tag{8}$$

where σ is the standard deviation of the logarithms of the grain sizes.

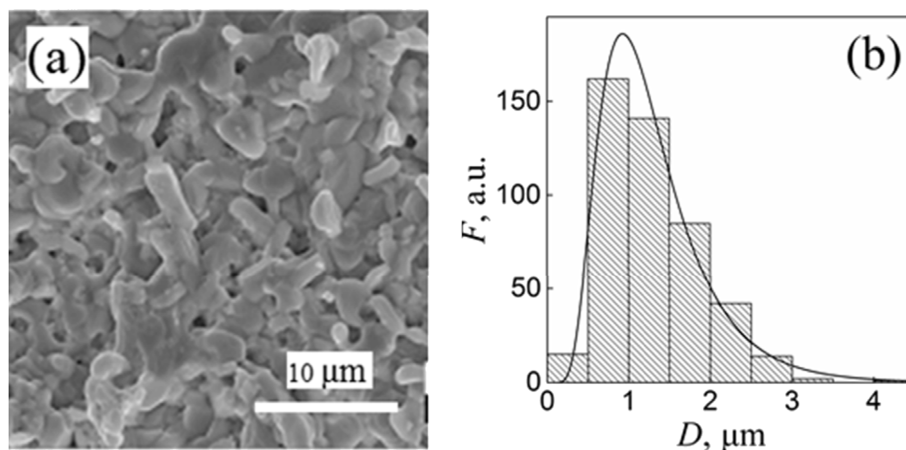

Fig. 5. (a) - The SEM image taken on the fractured surface; (b) – The histogram of the grain size distribution.

The standard deviation is measure of the width of the distribution. One can see that expression (8) reproduces the experimental grain size distribution very well. By fitting this distribution, the values of $\overline{D}$ and σ were estimated as ~1160 nm and ~0.46, respectively. The estimated $\overline{D}$ value is bigger as compared to the highest l value calculated for $Bi_{1.9}Lu_{0.1}Te_3$ (Table 1, $l \approx 1730$ nm at $T = 2.8$ K and $E = 0.15$ V·m^{-1}). However, $\overline{D}$ is the average grain size. A sufficient fraction of the grains with $D > \overline{D}$ can be also found in the histogram in Fig. 5 (b). So, a suggested relation between D and maximum l value can be really existed.

The minimum l value should be limited by a distance between the nearest Lu atoms. The Bi_2Te_3 crystal consists of 15 layers stacked along the c-axis and presents a combination of three hexagonal layer stacks of the composition in which each set consists of five atoms (Te_1–Bi–Te_2–Bi–Te_1) [29]. Let us take into account that there are three formula units per trigonal unit cell of the Lu-doped Bi_2Te_3 compounds. According to Ref. [30], at room temperature the a and c parameters of the unit cell are equal to 4.388 Å and 30.481 Å, respectively. As was mentioned above, the Lu content in the sample studied is 1.98 at%. It means that almost each fiftieth Bi atom is substituted for the Lu atom. Then, the distance between the nearest Lu atoms can be estimated as ~25 nm. This value is less as compared to the least a value calculated for $Bi_{1.9}Lu_{0.1}Te_3$ (Table 1, $l \approx 110$ nm at $T = 6.5$ K and $E = 1.46$ V·m^{-1}).

Thus, on the one hand, the l estimates are in agreement with two specific sizes important for the VRH conductivity. But, on the other hand, the l values estimated for $Bi_{1.9}Lu_{0.1}Te_3$ in this work seem to be too big as compared to the average hopping distance estimated for other materials with the VRH conductivity (≈20 nm in CdSb single crystal doped 2 at% Ni [25], ≈14 nm at electric field of 100 V·m^{-1} in $PrBa_2Cu_3O_{7-\delta}$ films [26], ≈6 nm in $CuGaSe_2$ films [31]).

To explain this contradiction, the magnetoresistance peculiarities recently found in $Bi_{1.9}Lu_{0.1}Te_3$ and characteristic for strongly disordered and inhomogeneous semiconductors should be considered. The main peculiarity is related to appearance of linear-in-magnetic field contribution to the total transverse and longitudinal magnetoresistance of $Bi_{1.9}Lu_{0.1}Te_3$, which is reflected in a crossover from quadratic magnetoresistance (at low magnetic fields) to linear magnetoresistance (at high magnetic fields), when magnetic field increases [32–34]. For instance, the magnetic field dependences of the transverse and longitudinal magnetoresistance, $\rho(B)/\rho(0)$, for $Bi_{1.9}Lu_{0.1}Te_3$ taken at temperature of 2 K are shown in Fig. 6. Here, $\rho(B)$ is the specific electrical resistivity at magnetic field B changing from 0 up to 45 T, and $\rho(0)$ is the specific electrical resistivity at zero magnetic field. Magnetic field was applied perpendicular to current direction to measure the transverse magnetoresistance, while parallel orientation of magnetic field and current direction was used to measure the longitudinal

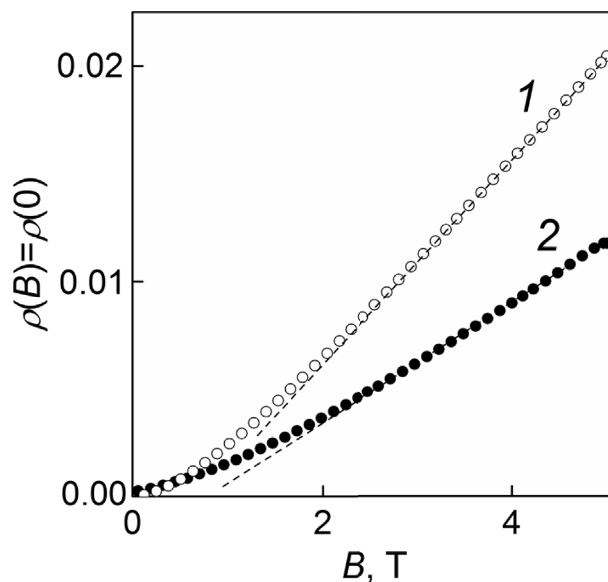

Fig. 6. The transverse (curve *1*) and longitudinal (*2*) $\rho(B)/\rho(0)$ vs. B dependences taken at temperature of 2 K.

magnetoresistance. Results of detailed magnetoresistance examination of Lu-doped Bi_2Te_3 will be published elsewhere.

The linear magnetoresistance can result from the Hall resistance picked up from macroscopically distorted current paths due to, in turn, local variations in the specific electrical resistivity of the compound studied [35–37]. That is in the disordered and inhomogeneous semiconductors the strong magnetic field can force a significant portion of the dc current to flow in a direction perpendicular to the applied voltage. Such kind of semiconductors can be considered as compounds consisting from numerous domains having various values of ρ. In this case, the local E values inside the domains with high ρ value can be much more as compared to the E values for the domains with high enough conductivity. In turn, higher E values used to estimate the l values will decrease the l estimates.

There are a few reasons resulting in electrical inhomogeneity of $Bi_{1.9}Lu_{0.1}Te_3$. First, in grained materials like $Bi_{1.9}Lu_{0.1}Te_3$, the grains are high-conductance domains, while the grain boundaries have a low conductivity. Second, for heavily doped semiconductors like $Bi_{1.9}Lu_{0.1}Te_3$ the spatial inhomogeneities differing in ρ can be resulted from the clustering of dopant atoms at lattice defects or grain boundaries that in turn will induce a local change in stoichiometry due to either excess or deficient of dopant atoms within the spatial

inhomogeneities. Such mechanism was developed for silver chalcogenides, Ag_2Se and Ag_2Te [36]. It should be noted that the exact distribution of the inhomogeneties can be difficult to resolve experimentally by either scattering or imaging techniques due to both a weak enough deviation of inhomogeneity stoichiometry from macroscopic stoichiometry and small size of the inhomogeneities. But, in this case the linear magnetoresistance can be served as an effective probe of the spatial conductivity distribution in the strongly disordered semiconductors.

The E values used in our analysis are really average electric fields for whole volume of the sample. No local E variations due to electrical inhomogeneity of the compound studied takes into account. In this case, too big $l(T, E)$ estimates extracted in our work can be probably attributed to incorrect and low E values. However, the quality dependences of the E-effect on the VRH conductivity will be the same.

4. Conclusion

Thus, the electric field effect on the variable-range hopping conductivity observed in n-type $Bi_{1.9}Lu_{0.1}Te_3$ at low temperatures was observed and studied in details. It was found that the average hopping distance decreases as temperature or electric field strength increase. So, both thermal activation and electric field activation should be taken into account to analyze the $Bi_{1.9}Lu_{0.1}Te_3$ conductivity. Rapid enhancement of the density of states at the Fermi level with increasing electric field was also found. This enhancement could be attributed to the impurity band originated from the electronic f-levels of Lu and having high and sharp density of states.

Declarations of interest

None.

Acknowledgements

O. I. thanks the Ministry of Education and Science of the Russian Federation for the financial support under project No 3.6586.2017/6.7. All of studies were carried out by the scientific equipment of joint research center “Technologies and Materials” at the Belgorod State University.

References

[1] Y. Pan, T.R. Wei, C.F. Wu, J.F. Li, J. Mater. Chem. C 3 (2015) 10583.
[2] L. Hu, T. Zhu, X. Liu, X. Zhao, Adv. Funct. Mater. 24 (2014) 5211.
[3] J. Suh, K.M. Yu, D. Fu, X. Liu, F. Yang, J. Fan, D.J. Smith, Y.H. Zhang, J.K. Furdyna, C. Dames, W. Walukiewicz, J. Wu, Adv. Mater. 27 (2015) 3681.
[4] X.K. Duan, K.G. Hu, D.H. Ma, W.N. Zhang, Y.Z. Jiang, S.C. Guo, Rare Met. 34 (2015) 770.
[5] D. Pascal Gehring, A. Gaul, A. Hoyer, K. Vaklinova, R.J. Mehta, M. Burghard, T. Borca-Tasciuc, D.J. Singh, K. Kern, G. Ramanath, Adv. Mater. 28 (2016) 6436.
[6] H.J. Goldsmid, J. Electron. Mater. 41 (2012) 2126.
[7] J.P. Heremans, V. Jovovic, E.S. Toberer, A. Saramat, K. Kurosaki, A. Charoenphakdee, S. Yamanaka, G.J. Snyder, Science 321 (2008) 554.
[8] B. Wiendlocha, J. Electron. Mater. 45 (2016) 3515.
[9] J. Yang, F. Wu, Z. Zhu, L. Yao, H. Song, X. Hu, J. Alloy. Comp. 40 (2015) 619.
[10] X.H. Ji, X.B. Zhao, Y.H. Zhang, B.H. Lu, H.L. Ni, J. Alloy. Comp. 387 (2005) 282.
[11] F. Wu, H. Song, J. Jia, X. Hu, Prog. Nat. Sci. Mater. Int. 23 (2013) 408.
[12] F. Wu, W. Shi, X. Hu, Electron. Mater. Lett. 11 (2015) 127.
[13] X.H. Ji, X.B. Zhao, Y.H. Zhang, B.H. Lu, H.L. Ni, Mater. Lett. 59 (2005) 682.
[14] F. Wu, H.Z. Song, J.F. Jia, F. Gao, Y.J. Zhang, X. Hu, Phys. Status Solidi (a) 210 (2013) 1183.
[15] X.B. Zhao, Y.H. Zhang, X.H. Ji, Inorg. Chem. Commun. 7 (2004) 386.
[16] M. Yaprintsev, R. Lyubushkin, O. Soklakova, O. Ivanov, J. Electron. Matter 47 (2018) 1362.
[17] O. Ivanov, M. Yaprintsev, Mater. Res. Express 5 (2018) 015905.
[18] O. Ivanov, M. Yaprintsev, R. Lyubushkin, O. Soklakova, Scripta Mater. 146 (2018) 91.
[19] T.E. Hupphrey, H. Linke, Phys. Rev. Lett. 94 (2005) 096601.
[20] G.D. Mahan, J.O. Sofo, Pros. Natl. Acad. Sci. USA 93 (1996) 7436.
[21] M.D. Daybell, W.A. Steyert, Rev. Mod. Phys. 40 (1968) 380.
[22] B.I. Shklovskii, A.L. Efros, Electronic Properties of Doped Semiconductor, Springer, Berlin, 1984.
[23] O. Ivanov, M. Yaprintsev, Solid State Sci. 76 (2018) 111.
[24] R. Laiho, A.V. Lashkul, K.G. Lisunov, E. Lahderanta, M.A. Shakhov, V.S. Zakhvalinskii, J. Phys.: Condens. Mater. 20 (2008) 295204.
[25] R. Laiho, K.G. Lisunov, E. Lahderanta, P.A. Petrenko, J. Salminen, M.A. Shakhov, M.O. Safontchik, V.S. Stamov, M.V. Shybnikov, V.S. Zakhvalinskii, J. Phys.: Condens. Mater. 14 (2002) 8043.
[26] G.K. van Ancum, M.A.J. Verhoeven, D.H.A. Blank, H. Rogalla, Phys. Rev. B 52 (1995) 5598.
[27] W. Richter, H.K. Köhler, C.R. Becker, Status Solidi (b) 84 (1977) 619.
[28] F.J. Humphreys, M. Hatherly, Recrystallization and Related Annealing Phenomena, Elsevier, Oxford, UK, 2004.
[29] G.S. Nolas, J. Sharp, H.J. Goldsmid, Thermoelectrics Basic Principles and New Materials Developments, Springer, Berlin, 2001.
[30] M. Yaprintsev, R. Lyubushkin, O. Soklakova, O. Ivanov, J. Electron. Mater. 47 (2018) 1362.
[31] E. Arushanov, S. Siebentritt, T. Schedel-Niedrg, M. Ch Lux-Steiner, J. Appl. Phys. 100 (2016) 063715.
[32] R. Xu, A. Husmann, T.F. Rosenbaum, M.L. Saboungi, J.E. Enderby, P.B. Littlewood, Nature 390 (1997) 57.
[33] A. Husmann, J.B. Betts, G.S. Boebinger, A. Migliori, T.F. Rosenbaum, M.L. Saboungi, Nature 417 (2002) 421.
[34] J. Hu, T.F. Rosenbaum, Nature Mater. 697 (2008) 7.
[35] M.M. Parish, P.B. Littlewood, Phys. Rev. B 72 (2005) 094417.
[36] J. Hu, T.F. Rosenbaum, Phys. Rev. B 75 (2007) 214203.
[37] M.M. Parish, P.B. Littlewood, Nature 426 (2003) 162.